

# EXPLOSION DEVELOPMENT IN A SPHERICAL VESSEL



UNITED STATES DEPARTMENT OF THE INTERIOR

BUREAU OF MINES

August 1969

# EXPLOSION DEVELOPMENT IN A SPHERICAL VESSEL

By John Nagy, John W. Conn, and Harry C. Verakis

\* \* \* \* \* report of investigations 7279



UNITED STATES DEPARTMENT OF THE INTERIOR  
Walter J. Hickel, Secretary

BUREAU OF MINES  
John F. O'Leary, Director

Nagy, John, 1913-

Explosion development in a spherical vessel, by John Nagy,  
John W. Conn, and Harry C. Verakis. [Washington] U.S. Dept.  
of the Interior, Bureau of Mines [1969]

23 p. illus. (U.S. Bureau of Mines. Report of investigations  
7279)

1. Explosions. 2. Mine explosions. I. Conn, John W., jt. auth.  
II. Verakis, Harry C., jt. auth. III. Title. (Series)

TN23.U7 no. 7279 622.06173

U.S. Dept. of the Int. Library

## CONTENTS

	<u>Page</u>
Abstract.....	1
Introduction.....	1
Flame development.....	3
Isothermal explosion in a spherical vessel.....	6
Adiabatic explosion in a spherical vessel.....	9
Correlation of theory and experiment.....	10
Discussion.....	17
Appendix A.--List of symbols.....	19
Appendix B.--Value of constants used in calculating explosion data.....	21
Appendix C.--Calculation of pressure-time and radius-time relations.....	22

## ILLUSTRATIONS

<u>Fig.</u>		
1.	Flame travel in an open-end tube.....	3
2.	Flame front in a segment of a spherical vessel.....	7
3.	Plot of experimental data according to equation 39.....	12
4.	Calculated and experimental data for flame radius and pressure during a 7.72-percent acetylene-air explosion in a spherical vessel.....	12
5.	Calculated and experimental data for flame radius and pressure during a moist carbon monoxide-oxygen explosion in a spherical vessel.....	13
6.	Calculated and experimental data for flame radius and time during a 7.72-percent acetylene-air explosion in a spherical vessel....	13
7.	Calculated and experimental data for flame radius and time during a moist carbon monoxide-oxygen explosion in a spherical vessel..	14
8.	Calculated and experimental data for pressure and time during a 7.72-percent acetylene-air explosion in a spherical vessel.....	15
9.	Calculated and experimental data for pressure and time during a moist carbon monoxide-oxygen explosion in a spherical vessel....	16
10.	Calculated and experimental data for pressure and time during an 0.8-oz/cu ft cornstarch dust explosion in a 110-cu-ft rectilinear chamber.....	16
C-1.	Integral evaluation by Simpson's rule for equations 30 and 37.....	23
C-2.	Integral evaluation by Simpson's rule for equations 32 and 38.....	23

# EXPLOSION DEVELOPMENT IN A SPHERICAL VESSEL

by

John Nagy,<sup>1</sup> John W. Conn,<sup>2</sup> and Harry C. Verakis<sup>3</sup>

---

## ABSTRACT

The Bureau of Mines examined explosion development in a closed spherical vessel, mathematically correlating flame travel, pressure, and time with parameters defining the reaction. The model assumes that burnt and unburnt zones are separated by a thin, radially moving flame front. Isothermal and adiabatic systems are considered. Correlation with gas and dust explosion data is better for the adiabatic system, but the isothermal development is simpler and in reasonably good agreement.

Interpretation of the explosion phenomena is facilitated by expressing the rate of mole change in the flame front in terms of elementary parameters. This expression is developed by examining the components of spatial-flame velocity.

## INTRODUCTION

During the past several decades, the Bureau of Mines has obtained considerable experimental information on dust explosion development in small-volume laboratory vessels,<sup>4</sup> in larger vented chambers,<sup>5</sup> and in the Experimental Coal

---

<sup>1</sup>Project coordinator, Dust and Ventilation.

<sup>2</sup>Research physicist, Dust and Ventilation.

<sup>3</sup>Chemist, Dust and Ventilation.

All authors are with the Health and Safety Research and Testing Center, Bureau of Mines, Pittsburgh, Pa.

<sup>4</sup>Dorsett, Henry G., Jr., Murray Jacobson, John Nagy, and Roger P. Williams. Laboratory Equipment and Test Procedures for Evaluating Explosibility of Dusts. BuMines Rept. of Inv. 5624, 1960, 21 pp.

Dorsett, Henry G., Jr., and John Nagy. Dust Explosibility of Chemicals, Drugs, Dyes, and Pesticides. BuMines Rept. of Inv. 7132, 1968, 23 pp.

Jacobson, Murray, Austin R. Cooper, and John Nagy. Explosibility of Metal Powders. BuMines Rept. of Inv. 6516, 1964, 25 pp.

Jacobson, Murray, John Nagy, and Austin R. Cooper. Explosibility of Dusts Used in the Plastics Industry. BuMines Rept. of Inv. 5971, 1962, 30 pp.

Jacobson, Murray, John Nagy, Austin R. Cooper, and Frank J. Ball. Explosibility of Agricultural Dusts. BuMines Rept. of Inv. 5753, 1961, 23 pp.

Nagy, John, Austin R. Cooper, and Henry G. Dorsett, Jr. Explosibility of Miscellaneous Dusts. BuMines Rept. of Inv. 7208, 1968, 31 pp.

Nagy, John, Henry G. Dorsett, Jr., and Austin R. Cooper. Explosibility of Carbonaceous Dusts. BuMines Rept. of Inv. 6597, 1965, 30 pp.

<sup>5</sup>Lartmann, Irving, and John Nagy. Recent Studies on Venting of Dust Explosions. Ind. and Eng. Chem., v. 49, October 1957, pp. 1734-1740.

Mine.<sup>6</sup> A mathematical model is required to correlate the numerous inter-related factors affecting explosion development in these volumes of diverse size and shape. Many researchers have studied explosion phenomena, and several mathematical models relating pressure and flame front with time are given in the literature. However, for the most part, these models are not amenable for mass flow in the vented vessels or in the open mine passageways. Therefore, an attempt has been made to develop a simplified model which permits incorporation of the mass-flow concept. As the first step toward this solution, a mathematical model is presented for explosion development in a closed spherical vessel. Because flame radius and time data are not available from experimental studies on dust explosions, the model is correlated with data published by others for acetylene-air,<sup>7</sup> and moist carbon monoxide-oxygen<sup>8</sup> mixtures. The developed equations are shown to be consistent with pressure-time observations for a cornstarch dust explosion in a 110-cubic-foot rectilinear vessel. Full agreement for the cornstarch dust explosion is not attained because the effects of the vessel size and shape, and the initial turbulence are yet to be resolved. Studies are now in progress to explain these factors.

As mathematical treatment of combustion phenomena and associated mass flow tends to become complex, the following simplifying assumptions, commonly used in combustion theory, are made:

1. The equation of state is  $PV = nRT$ ,<sup>9</sup> where  $P$  = absolute pressure,  $V$  = volume,  $n$  = number of moles,  $R$  = universal gas constant, and  $T$  = absolute temperature.
2. A quiescent uniform combustible mixture is ignited by a central spark or negligible energy and volume.
3. Viscosity and heat capacities are constant.
4. The flame-front velocity is low relative to the velocity of sound; thus pressure is uniform in the vessel.
5. The time of burning in the flame front is short, relative to the total time of the explosion; thus combustion is completed within a thin flame front.

---

<sup>6</sup>Hartmann, Irving. Studies on the Development and Control of Coal-Dust Explosions in Mines. BuMines Inf. Circ. 7785, 1957, 27 pp.

Nagy, John, Donald W. Mitchell, and Edward M. Kawenski. Float Coal Hazards in Mines: A Progress Report. BuMines Rept. of Inv. 6581, 1965, 15 pp.

<sup>7</sup>Rallis, C. J., A. M. Garforth, and J. A. Steinz. The Determination of Laminar Burning Velocity With Particular Reference to the Constant Volume Method: Part 3 - Experimental Procedure and Results. Univ. of the Witwatersrand, Johannesburg, Rept. 26, March 1965, 151 pp.

<sup>8</sup>Flock, E. F., C. F. Marvin, Jr., F. R. Caldwell, and C. H. Roeder. Flame Speeds and Energy Considerations for Explosions in a Spherical Bomb. National Advisory Committee on Aeronautics Rept. 682, 1940, 20 pp.

<sup>9</sup>Symbols are listed and identified in appendix A.

### FLAME DEVELOPMENT

The spatial-flame velocity is used in correlating the radial flame front and pressure with time. This spatial-flame velocity, designated as either  $dr/dt$  or  $S_s$ , is the vector sum of four components--a transformation velocity (burning velocity)  $S_t$ , characteristic of the reactivity of the constituents and their heat-transfer properties; a velocity component  $S_n$ , due to a change in the number of moles during the combustion process; a gas-expansion velocity  $S_e$ , due to thermal heating; and the initial velocity  $S_i$  of the gases. In the present instance, the gas is taken at rest and the initial velocity  $S_i$  is zero.

A physical interpretation of these four components of the spatial velocity is possible. In the hypothetical system shown in figure 1, a uniform fuel-air mixture is initially at rest in a tube open to the atmosphere at one end. The mixture is ignited at the closed end, and the flame travels toward the open end. For a short tube, the pressure  $P$  remains atmospheric; hence, all gas movement is toward the open end. The flame front is considered flat. The temperatures of the burnt and unburnt gases are  $T_b$  and  $T_u$ , respectively.

The transformation velocity  $S_t$ , often termed the burning velocity, is defined as the gas velocity normal to the flame front with which the unburnt mixture enters a stationary flame and is chemically transformed. The transformation velocity is illustrated by assuming the molecular weight and the temperature are not affected by the advancing flame (cool flame) in figure 1. During time  $\Delta t$ , the flame front advances by chemical transformation from  $x$  to  $x + \Delta x$  enveloping a mass of gas  $\Delta m$  that has an initial volume  $\Delta V_u$  and consists of  $\Delta n_u$  moles. Applying the equation of state to this incremental volume and dividing by the unit time interval,

$$\frac{\Delta V_u}{\Delta t} = \frac{RT_u}{P} \frac{\Delta n_u}{\Delta t}. \quad (1)$$

Since  $\Delta V_u = A\Delta x$  and  $S_t = \Delta x/\Delta t$ , where  $A$  is the area of the flame front, the expression for transformation flame velocity is

$$S_t = \frac{RT_u}{AP} \frac{\Delta n_u}{\Delta t}. \quad (2)$$

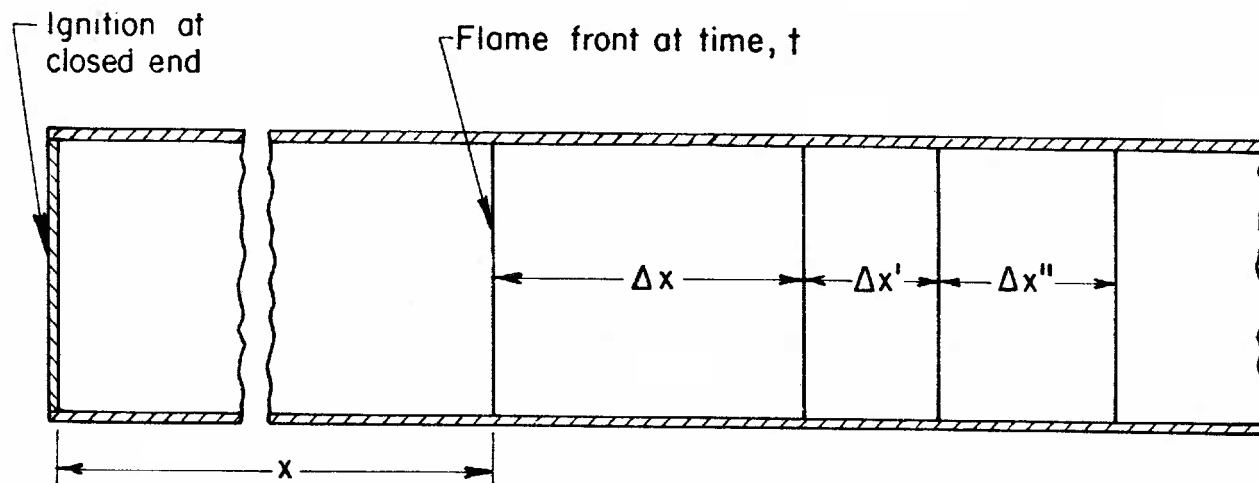


FIGURE 1. - Flame Travel in an Open-End Tube.

We next consider the velocity imparted to the flame front by a change in the average molecular weights of the unburnt and burnt gases and assume the temperature does not change during the reaction. From conservation of mass

$$\Delta m = \bar{M}_u \Delta n_u = \bar{M}_b \Delta n_b, \quad (3)$$

where  $\bar{M}_u$  and  $\bar{M}_b$  are the average molecular weights of the unburnt and burnt gases, respectively. During time  $\Delta t$ , the flame front advances as before from  $x$  to  $x + \Delta x$ , owing to the chemical transformation, and extends an additional distance to  $\Delta x'$  owing to the change in volume from an assumed increase in number of moles. If the number of moles of the products were less than that for the original mixture,  $\Delta x'$  would be negative. The incremental volume due to change in number of moles is

$$\Delta V' = A \Delta x', \quad (4)$$

or the rate of change is

$$\frac{\Delta V'}{\Delta t} = \frac{\Delta x + \Delta x'}{\Delta t} A - \frac{\Delta x}{\Delta t} A = \frac{RT_u}{P} \frac{\Delta n_b}{\Delta t} - \frac{RT_u}{P} \frac{\Delta n_u}{\Delta t}. \quad (5)$$

By using equation 3, the velocity due to the mole volume change is

$$S_n = \frac{\Delta x'}{\Delta t} = \frac{RT_u}{AP} \left( 1 - \frac{\bar{M}_b}{\bar{M}_u} \right) \frac{\Delta n_b}{\Delta t}. \quad (6)$$

Finally, to obtain the component of the spatial-flame velocity caused by thermal heating, it is assumed the reaction increases the temperature of the gases from  $T_u$  to  $T_b$ . The incremental volume due to this temperature change is

$$V'' = A \Delta x'', \quad (7)$$

and the volume rate increase derived in the same manner as equation 5 gives

$$\frac{\Delta V''}{\Delta t} = \frac{R}{P} (T_b - T_u) \frac{\Delta n_b}{\Delta t}. \quad (8)$$

The corresponding flame velocity caused by gas expansion is

$$S_e = \frac{\Delta x''}{\Delta t} = \frac{R}{AP} (T_b - T_u) \frac{\Delta n_b}{\Delta t}. \quad (9)$$

The components of the spatial-flame velocity were derived for a one-dimensional system. However, examination of a system for unconfined radial-flame development shows it to be equivalent if the linear  $x$  dimension is converted to  $r$ , the radial dimension. Thus, for flame development in a soap bubble,

$$S_s = S_t + S_n + S_e + S_1, \quad (10)$$

and, using equation 3,

$$S_s = \frac{RT_u}{AP} \frac{\bar{M}_b}{\bar{M}_u} \frac{\Delta n_b}{\Delta t} + \frac{RT_u}{AP} \left(1 - \frac{\bar{M}_b}{\bar{M}_u}\right) \frac{\Delta n_b}{\Delta t} + \frac{R}{AP} (T_b - T_u) \frac{\Delta n_b}{\Delta t} + 0, \quad (11)$$

which simplifies to

$$S_s = \frac{RT_b}{AP} \frac{\Delta n_b}{\Delta t}. \quad (12)$$

The spatial-flame velocity, equation 12, can be derived directly by differentiating the equation of state for the burnt zone  $PV_b = n_b RT_b$ , and by substituting  $A dr/dt = dV_b/dt$ . In this derivation, the velocity components are not explicit.

The equations for the velocity components can be simplified by expressing  $dn_b/dt$  in terms of elementary constants. In 1879, Gouy<sup>10</sup> postulated that the amount of gas ignited (or entering the flame front per unit time per unit area) is constant for a given pressure and temperature. Khitrin<sup>11</sup> states Gouy's postulate mathematically as

$$\frac{1}{A} \frac{\Delta V_u}{\Delta t} = k_r', \quad (13)$$

where  $k_r'$  is a constant having dimensions of velocity. The transformation velocity  $S_t$  and the constant  $k_r'$  are identical.

Experiments show  $k_r'$  varies with the temperature and pressure of the unburnt gas. Correlation of these parameters by theory<sup>12</sup> produces relatively complex equations. The experiments indicate  $k_r'$  varies approximately as the square of the absolute temperature<sup>13</sup> and inversely as a power function of the absolute pressure.<sup>14</sup> The exponent of the pressure term is related to the concentration and type of fuel in the system. If the exponent of the pressure function is zero, the burning velocity is independent of the pressure.

<sup>10</sup>Khitrin, L. H. The Physics of Combustion and Explosion. National Science Foundation, 1962, p. 128 (trans. from Russian); Office of Tech. Services, U.S. Dept. of Commerce, OTS 61-31205.

<sup>11</sup>Work cited in reference 10.

<sup>12</sup>Rallis, C. J., A. M. Garforth, and J. A. Steinz. Laminar Burning Velocity of Acetylene-Air Mixtures by the Constant-Volume Method. Combustion and Flame (London), v. 9, No. 4, December 1965, pp. 345-356.

Semenov, N. N. Thermal Theory of Combustion and Explosion. III. Theory of Normal Flame Propagation. Trans. NACA TM 1026, 1942, 73 pp.

Tanford, Charles, and Robert N. Pease. Theory of Burning Velocity. II. The Square Root Law for Burning Velocity. J. Chem. Phys., v. 15, No. 12, December 1947, pp. 861-865.

<sup>13</sup>Pages 147-156 of work cited in reference 10.

<sup>14</sup>Egerton, Alfred, and A. H. LeFebvre. Flame Propagation: The Effect of Pressure Variation on Burning Velocities. Proc. Roy. Soc., series A, v. 222, 1954, pp. 206-223.

These experimental findings on the effect of temperature and pressure on burning velocity can readily be consolidated with Gouy's postulate by relating the ambient temperature and pressure to respective values at a defined reference level. As burning velocities are most often determined at normal laboratory temperature and pressure, the reference levels can arbitrarily be defined to be  $T_r = 537^\circ \text{ R}$  ( $25^\circ \text{ C}$ ) and  $P_r = 14.7 \text{ psia}$ . The combined expression then becomes

$$\frac{1}{A} \frac{\Delta V_u}{\Delta t} = k_r \left( \frac{T_u}{T_r} \right)^2 \left( \frac{P_r}{P} \right)^\beta, \quad (14)$$

where  $T_u$  and  $P$  are the temperature and pressure of the unburnt gas,  $\beta$  is an exponent indicating the dependence of the rate of reaction on pressure, and  $k_r$  is the burning velocity at the reference level. When the temperature and pressure of the unburnt gas are at the reference levels, equations 13 and 14 are identical.

The rate of volume change per unit area of flame front is equated to an equivalent rate of mole change per unit area from the equation of state, or

$$\frac{1}{A} \frac{\Delta V_u}{\Delta t} = \frac{RT_u}{AP} \frac{\Delta n_u}{\Delta t} = k_r \left( \frac{T_u}{T_r} \right)^2 \left( \frac{P_r}{P} \right)^\beta. \quad (15)$$

By applying equation 3, the rate of mole change of burnt gas is defined as

$$\frac{dn_b}{dt} = k_r \frac{T_u}{T_r^2} \frac{AP}{R} \frac{\bar{M}_u}{\bar{M}_b} \left( \frac{P_r}{P} \right)^\beta. \quad (16)$$

By substituting equation 16 into equations 12, 2, 6, and 9, the spatial, transformation, mole change, and gas expansion velocities for flame development in a soap bubble become

$$S_s = k_r \frac{T_u T_b}{T_r^2} \frac{\bar{M}_u}{\bar{M}_b} \left( \frac{P_r}{P} \right)^\beta. \quad (17)$$

$$S_t = k_r \left( \frac{T_u}{T_r} \right)^2 \left( \frac{P_r}{P} \right)^\beta. \quad (18)$$

$$S_n = k_r \left( \frac{T_u}{T_r} \right)^2 \left( \frac{\bar{M}_u}{\bar{M}_b} - 1 \right) \left( \frac{P_r}{P} \right)^\beta. \quad (19)$$

$$S_e = k_r \frac{T_u (T_b - T_u)}{T_r^2} \frac{\bar{M}_u}{\bar{M}_b} \left( \frac{P_r}{P} \right)^\beta. \quad (20)$$

#### ISOTHERMAL EXPLOSION IN A SPHERICAL VESSEL

The model for an isothermal system which follows is presented because the equations are relatively simple and in some instances, for example, where the number of moles in a vented vessel is a factor, appear to be sufficiently definitive. In a closed vessel where relatively high pressures are produced,

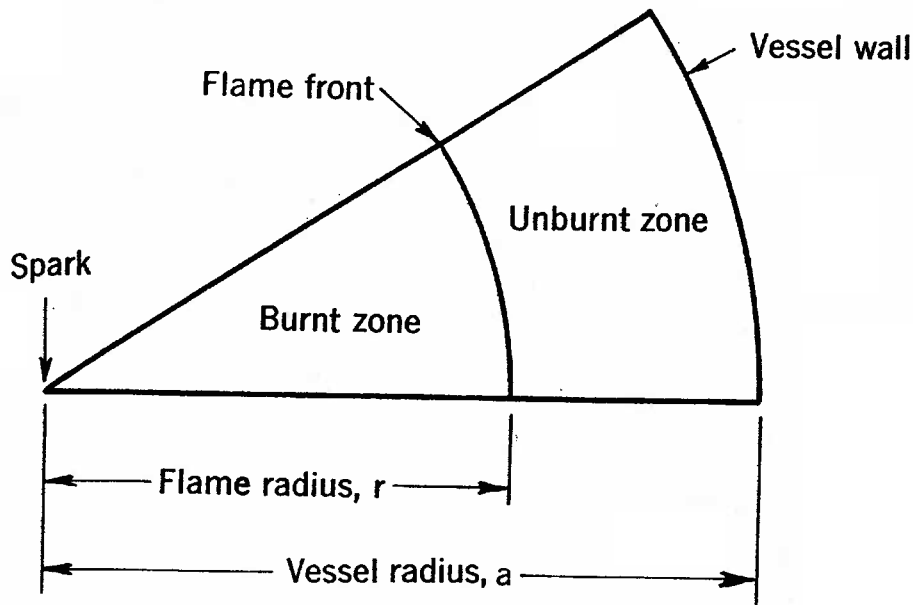


FIGURE 2. - Flame Front in a Segment of a Spherical Vessel.

equations developed by considering an adiabatic system give better agreement with experimental results.

In a spherical vessel (fig. 2), the pressure and spatial-flame velocity are not constant as in a soap-bubble experiment. A thin spherical-flame front divides the gas into burnt and unburnt zones. The pressure is considered uniform throughout the vessel. For the isothermal process, the temperature of the unburnt gas  $T_u$  is constant and

equals  $T_o$ , the initial temperature. The temperature of the burnt gas  $T_b$  is also constant and equals  $T_m$ , the maximum temperature attained during the reaction. In subsequent development for the adiabatic system, distinction is made between  $T_o$  and  $T_u$ , and between  $T_m$  and  $T_b$ .

For the nonturbulent system, relations between flame radius, mass, pressure, and time may be derived from equation 16 and the following equations:

$$PV_b = n_b RT_b, \quad (21)$$

and

$$PV_u = n_u RT_u, \quad (22)$$

$$m = \bar{M}_u n_u + \bar{M}_b n_b, \quad (23)$$

where  $m$  is the total mass of gas in the vessel. At the beginning and end of the explosion, the respective equations of state are

$$P_o V = \frac{m}{\bar{M}_u} RT_o, \quad (24)$$

and

$$P_m V = \frac{m}{\bar{M}_b} RT_m, \quad (25)$$

where  $P_o$  and  $P_m$  are the initial and final pressures in the vessel. The relation between temperature and pressure is obtained by dividing equations 24-25 to produce

$$\frac{P_o}{P_m} = \frac{\bar{M}_b T_o}{\bar{M}_u T_m}. \quad (26)$$

The relation between the rates of mole change, obtained by differentiating equation 23, is

$$\frac{dn_b}{dt} = - \frac{\bar{M}_u}{\bar{M}_b} \frac{dn_u}{dt}. \quad (27)$$

The flame radius correlated with pressure, using equations 21-23 and 26 is

$$r^3 = a^3 \frac{1 - \frac{P_o}{P}}{1 - \frac{P_o}{P_m}}, \quad (28)$$

where  $r$  is the flame radius and  $a$  is the vessel radius.

The expression for spatial-flame velocity is obtained by using equation 28 to eliminate  $P$  in equation 21, differentiating with respect to time, and applying equations 16 and 26-27 to give

$$\frac{dr}{dt} = \frac{k_r T_o^2 P_r^\beta P_m}{T_r^2} \frac{1}{P^{1+\beta}}. \quad (29)$$

The pressure term in equation 29 may be expressed as a function of the radius, using equation 28 to give

$$\frac{dr}{dt} = \frac{k_r T_o^2 P_r^\beta P_m}{T_r^2 P_o^{1+\beta}} \left[ 1 - \left( 1 - \frac{P_o}{P_m} \right) \frac{r^3}{a^3} \right]^{1+\beta}. \quad (30)$$

The expression for rate of pressure development is obtained by adding equations 21 and 22, differentiating with respect to time, and applying equations 16 and 26-27. Thus,

$$\frac{dP}{dt} = \frac{3k_r T_o^2 P_r^\beta}{a^3 T_r^2 P_o} (P_m - P_o) r^2 P^{1-\beta}. \quad (31)$$

Using equation 28 the radius term in equation 31 is expressed as a function of the pressure to give

$$\frac{dP}{dt} = \frac{3k_r T_o^2 P_r^\beta P_m^{2/3}}{a T_r^2 P_o} (P_m - P_o)^{1/3} \left( 1 - \frac{P_o}{P} \right)^{2/3} P^{1-\beta}. \quad (32)$$

Equations 30 and 32 can be integrated when  $\beta$  equals zero by transformation to the following standard form appearing in most tables of integrals:

$$\int_0^X \frac{dX}{A+BX^3} = \frac{C}{3A} \left[ \frac{1}{2} \ln \frac{(c+X)^2}{c^2 - cX + X^2} + \sqrt{3} \tan^{-1} \frac{2X-c}{c\sqrt{3}} + \sqrt{3} \tan^{-1} \frac{1}{\sqrt{3}} \right] = Dt, \quad (33)$$

where  $C = \left( \frac{A}{B} \right)^{1/3}$ .

For equation 30,

$$\chi = \frac{r}{a}, A = 1, B = -\left(1 - \frac{P_o}{P_m}\right), \text{ and } D = \frac{k_r T_o^2 P_m}{T_r^2 P_o},$$

and for equation 32,

$$\chi = \left(1 - \frac{P_o}{P}\right)^{1/3}, A = 1, B = -1, \text{ and } D = \frac{3k_r T_o^2 P_m^{2/3}}{a T_r^2 P_o} (P_m - P_o)^{1/3}.$$

#### ADIABATIC EXPLOSION IN A SPHERICAL VESSEL

Equations for an adiabatic, nonturbulent system are derived in a manner similar to that for the isothermal system. However, the average temperatures in the burnt and unburnt zones now are not constant but are related to the degree of compression. In accordance with adiabatic pressure changes, the relations between temperatures and pressures are

$$T_u = T_o \left(\frac{P}{P_o}\right)^{1-1/\gamma_u}, \quad (34)$$

and

$$T_b = T_m \left(\frac{P}{P_m}\right)^{1-1/\gamma_b}, \quad (35)$$

where  $\gamma_u$  and  $\gamma_b$  are the ratios of specific heats at constant pressure and volume for the unburnt and burnt gases. Although equations can be developed using separate values for  $\gamma_u$  and  $\gamma_b$ , for simplicity, we assume an average value of  $\gamma$  for the system. When separate values for  $\gamma$  are used, better agreement is obtained between theory and experiment, but the equations become unwieldy. The calculations and curves presented in this paper indicate that the use of the average  $\gamma$  does not introduce a serious error.

Using the same procedures as for the isothermal system, but considering  $T_u$  and  $T_b$  as functions of the pressure, the following equations are derived for the adiabatic system:

$$r^3 = a^3 \frac{1 - \left(\frac{P_o}{P}\right)^{1/\gamma}}{1 - \left(\frac{P_o}{P_m}\right)^{1/\gamma}}, \quad (36)$$

$$\frac{dr}{dt} = \frac{k_r T_o^2 P_r^{\beta} P_m^{1/\gamma}}{T_r^2 P_o^{1/\gamma+\beta}} \left\{ 1 - \left[ 1 - \left(\frac{P_o}{P_m}\right)^{1/\gamma} \right] \frac{r^3}{a^3} \right\}^{3-2/\gamma+\beta\gamma}, \quad (37)$$

$$\frac{dP}{dt} = \frac{3\gamma k_r T_o^2 P_r^{\beta} P_m^{2/3\gamma}}{a T_r^2 P_o^{2-1/\gamma}} (P_m^{1/\gamma} - P_o^{1/\gamma})^{1/3} \left[ 1 - \left(\frac{P_o}{P}\right)^{1/\gamma} \right]^{2/3} P^{3-2/\gamma-\beta}. \quad (38)$$

Equations 37-38 cannot be integrated directly, but can be evaluated by approximation methods.

## CORRELATION OF THEORY AND EXPERIMENT

The following constants are introduced in deriving the equations for explosion development:

- $a$  - radius of vessel.
- $\gamma$  - ratio of specific heats of the gas at constant pressure to constant volume.
- $k_r$  - reaction rate constant (burning velocity) at the reference level of temperature and pressure.
- $\bar{M}_u, \bar{M}_b$  - average molecular weights of unburnt and burnt gases.
- $\beta$  - exponent indicating dependence of transformation velocity on pressure.
- $P_m$  - final explosion pressure.
- $P_o$  - initial pressure.
- $P_r$  - reference pressure level, 14.7 psia.
- $R$  - universal gas constant.
- $T_o$  - initial temperature.
- $T_r$  - reference temperature level, 537° R.

Values of the constants  $a$ ,  $P_o$ , and  $T_o$  are easily obtained to a high degree of accuracy. An average value of  $\gamma$  for the system can be estimated from the theoretical calculated values of  $\gamma_u$  and  $\gamma_b$ . The maximum pressure  $P_m$  can be obtained by experiment, or from calculated explosion temperatures.<sup>15</sup>

For the 7.72-percent acetylene-air mixture,<sup>16</sup> the maximum pressure by experiment is 100.8 psia, and from calculation, 135.4 psia. The difference presumably is due to heat loss to the vessel wall. The value of  $\beta$  for a few combustible gas mixtures can be found in the literature;<sup>17</sup> for most mixtures, it is 0.5 or less. When the initial temperature and pressure of the unburnt mixture are at normal room conditions, the constant  $k_r$  and the transformation velocity (burning velocity)  $S_t$  are identical. Values of  $S_t$  for most gas mixtures can be found in the literature.<sup>17</sup>

---

<sup>15</sup>Glasstone, Samuel. Thermodynamics for Chemists. D. Van Nostrand Co., Inc., New York, 1954, pp. 84-89.

Goodenough, G. A., and G. T. Felbeck. An Investigation of the Maximum Temperatures and Pressures Attainable in the Combustion of Gaseous and Liquid Fuels. Univ. of Illinois Bull. 139, March 1924, 160 pp.

Steffensen, R. J., J. T. Agnew, and R. A. Olsen. Combustion of Hydrocarbons: Property Tables. Purdue Univ. Eng. Ext. Series, No. 122, May 1966, 98 pp.

<sup>16</sup>Work cited in reference 7.

<sup>17</sup>Lewis, Bernard, and Guenther von Elbe. Combustion, Flames and Explosions of Gases. Academic Press Inc., New York, 2d ed., 1961, 731 pp.

The value of  $\beta$  and  $k_r$  can also be determined from either the adiabatic radius-time or pressure-time data of a closed-vessel explosion. Equation 38 in log form states:

$$\log \frac{\frac{dP}{dt}}{\left[1 - \left(\frac{P_0}{P}\right)^{1/\gamma}\right]^{2/3}} = \log k_1 + \left(3 - \frac{2}{\gamma} - \beta\right) \log P, \quad (39)$$

$$\text{where } k_1 = \frac{3\gamma k_r T_0^2 P_r \beta P_m^{2/3\gamma}}{a T_r^2 P_0^{2-1/\gamma}} (P_m^{1/\gamma} - P_0^{1/\gamma}).$$

Figure 3 shows acetylene-air explosion data (circles) plotted according to equation 39. The values of  $\beta$  and  $k_r$  are obtained from the slope and intercept of the curve, respectively.

Examination of the experimental data of Rallis and Fiock<sup>18</sup> shows that the constants  $\beta$  and  $k_r$  cannot be calculated accurately in a similar manner from the equivalent isothermal equation 32. This is to be expected since the isothermal model is only an approximation.

The values of the several constants used in correlating the developed equations with experimental data are listed in appendix B.

For the isothermal calculations,  $\beta$  was chosen as zero and  $k_r$  was calculated from the slope of equation 32 plotted on Cartesian coordinates as  $dP/dt$  versus  $(1 - P_0/P)^{2/3} P$ . If the value of  $\beta$  is known from experimental data, a more accurate isothermal value of  $k_r$  can be calculated. Equations 30, 32, and 37-38 were integrated using Simpson's rule; these data are given in appendix C.

Correlation of flame radius and pressure for the isothermal and the adiabatic system is shown in figure 4. The solid circles represent data reported by Rallis<sup>19</sup> for a 7.72-percent acetylene-air mixture. Calculated isothermal values, equation 28, are shown by the dashed line, and the adiabatic values, equation 36, by the solid line. Figure 5 shows data obtained by Fiock<sup>20</sup> for a mixture of oxygen with 2.69 percent water and 64.87 percent carbon monoxide. In both instances, agreement between experimental data and calculated adiabatic values is better than for the isothermal system.

Figure 6 shows flame radius-time data for the acetylene-air explosion and figure 7 shows similar data for the carbon monoxide-oxygen explosion. Agreement between the calculated adiabatic values and experimental data is good.

Figures 8 and 9 show experimental data and calculated curves for the pressure-time relation. The isothermal values are calculated using equation 32 and the adiabatic values using equation 38. The agreement between theory and experiment is good except near the end of the acetylene-air explosion,

---

<sup>18</sup>Works cited in references 7 and 8.

<sup>19</sup>Work cited in reference 7.

<sup>20</sup>Work cited in reference 8.

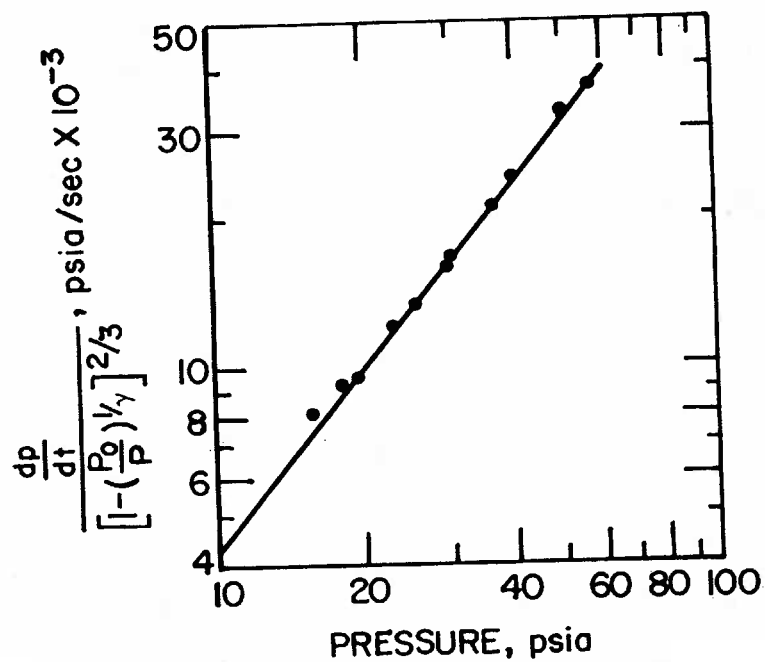


FIGURE 3. - Plot of Experimental Data According to Equation 39.

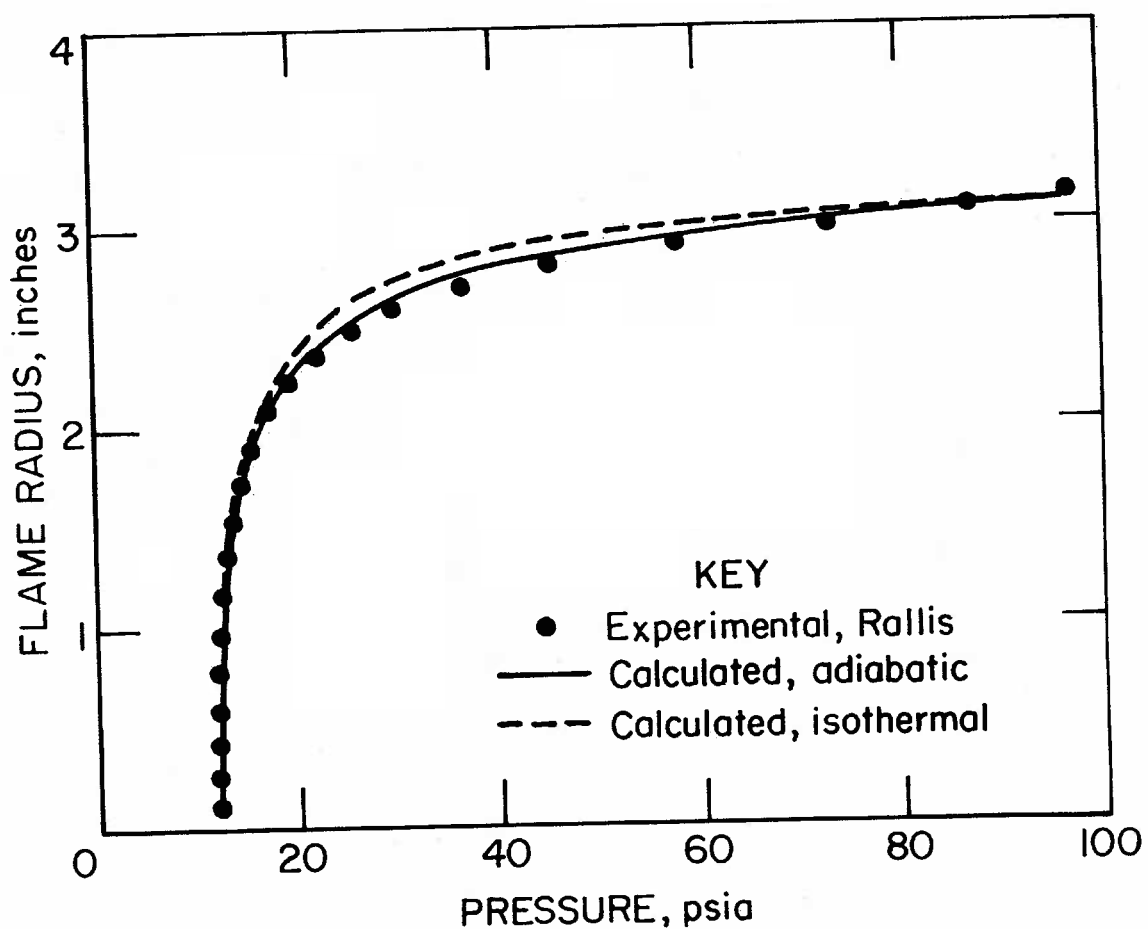


FIGURE 4. - Calculated and Experimental Data for Flame Radius and Pressure During a 7.72-Percent Acetylene-Air Explosion in a Spherical Vessel.

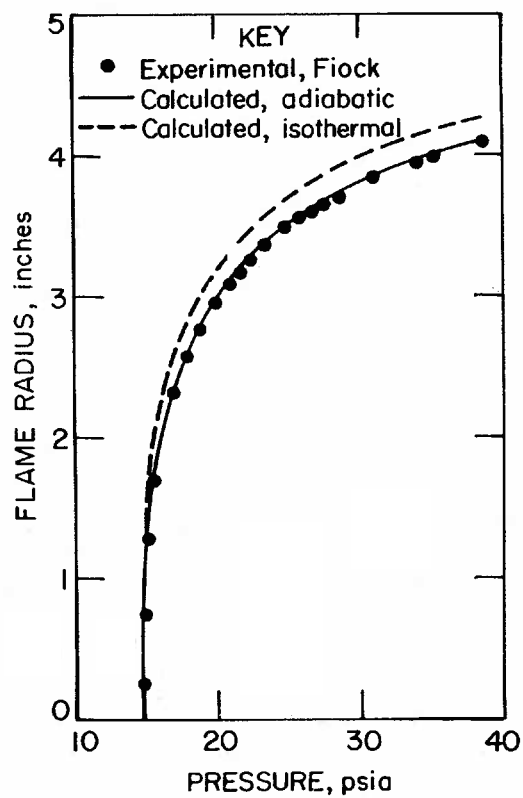


FIGURE 5. - Calculated and Experimental Data for Flame Radius and Pressure During a Moist Carbon Monoxide-Oxygen Explosion in a Spherical Vessel.

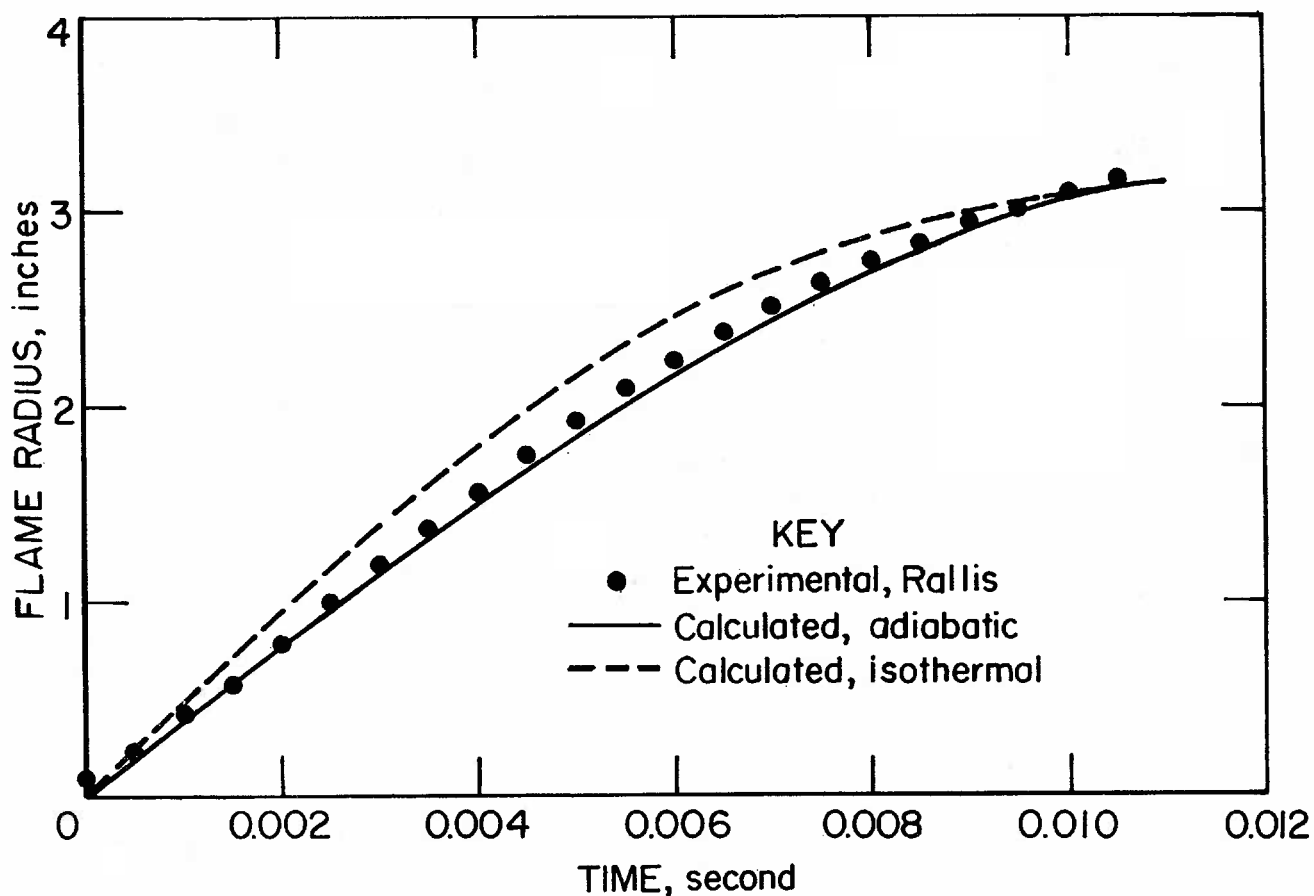


FIGURE 6. - Calculated and Experimental Data for Flame Radius and Time During a 7.72-Percent Acetylene-Air Explosion in a Spherical Vessel.

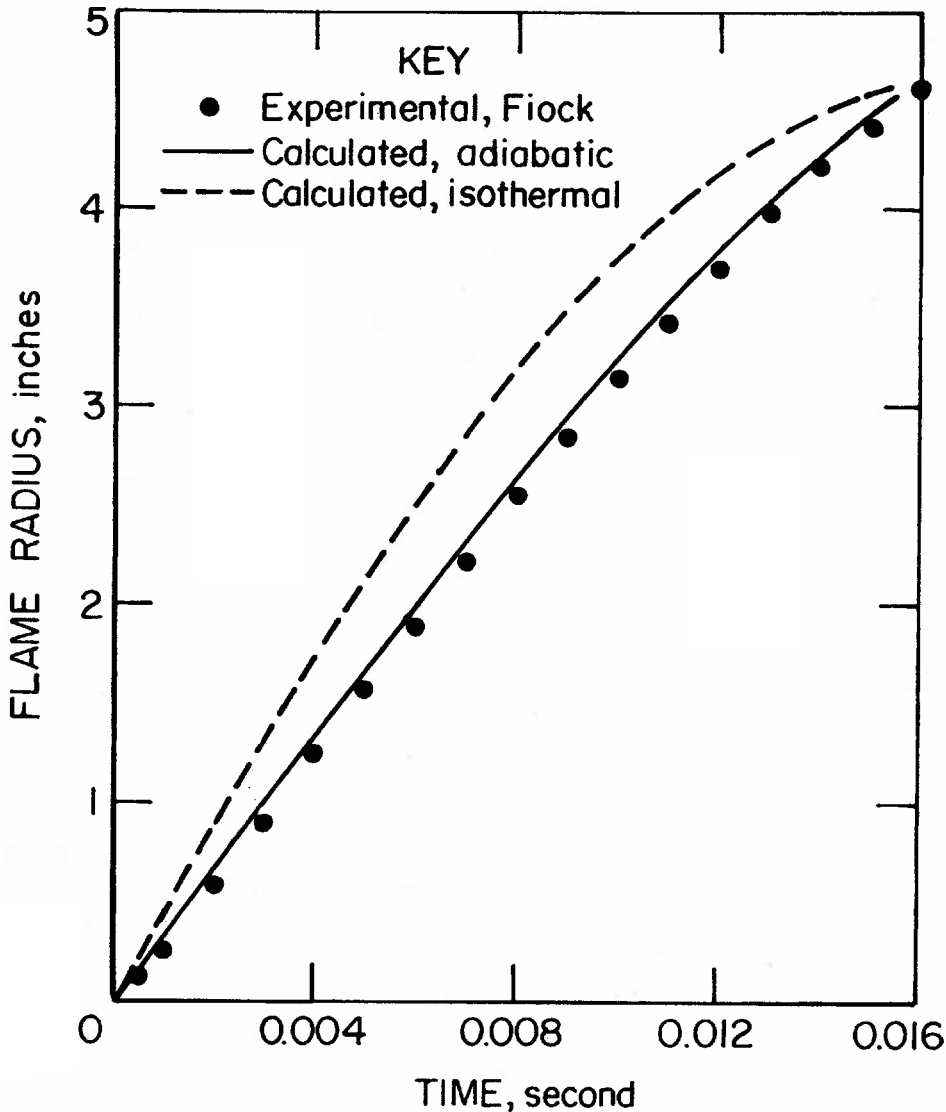


FIGURE 7. - Calculated and Experimental Data for Flame Radius and Time During a Moist Carbon Monoxide-Oxygen Explosion in a Spherical Vessel.

where the experimental data are presumably affected by heat losses and a finite amount of time for combustion in the flame front. Divergence between theory and experiment at the end of the explosion could not be evaluated for carbon monoxide-oxygen because pressure data are given only to about 40 psia. The curves presented are for stoichiometric fuel-air and fuel-oxygen mixtures. The agreement for other fuel-air ratios is almost as good, except for extremely lean or rich mixtures.

Calculated and experimental values for pressure development for a corn-starch dust explosion in a 110-cu-ft rectilinear vessel are given in figure 10. The circles are the experimentally measured values, the dashed line is calculated assuming an isothermal system, and the solid line is calculated assuming an adiabatic system. As for the gas explosions, agreement between experiment and calculation is better for the adiabatic system.

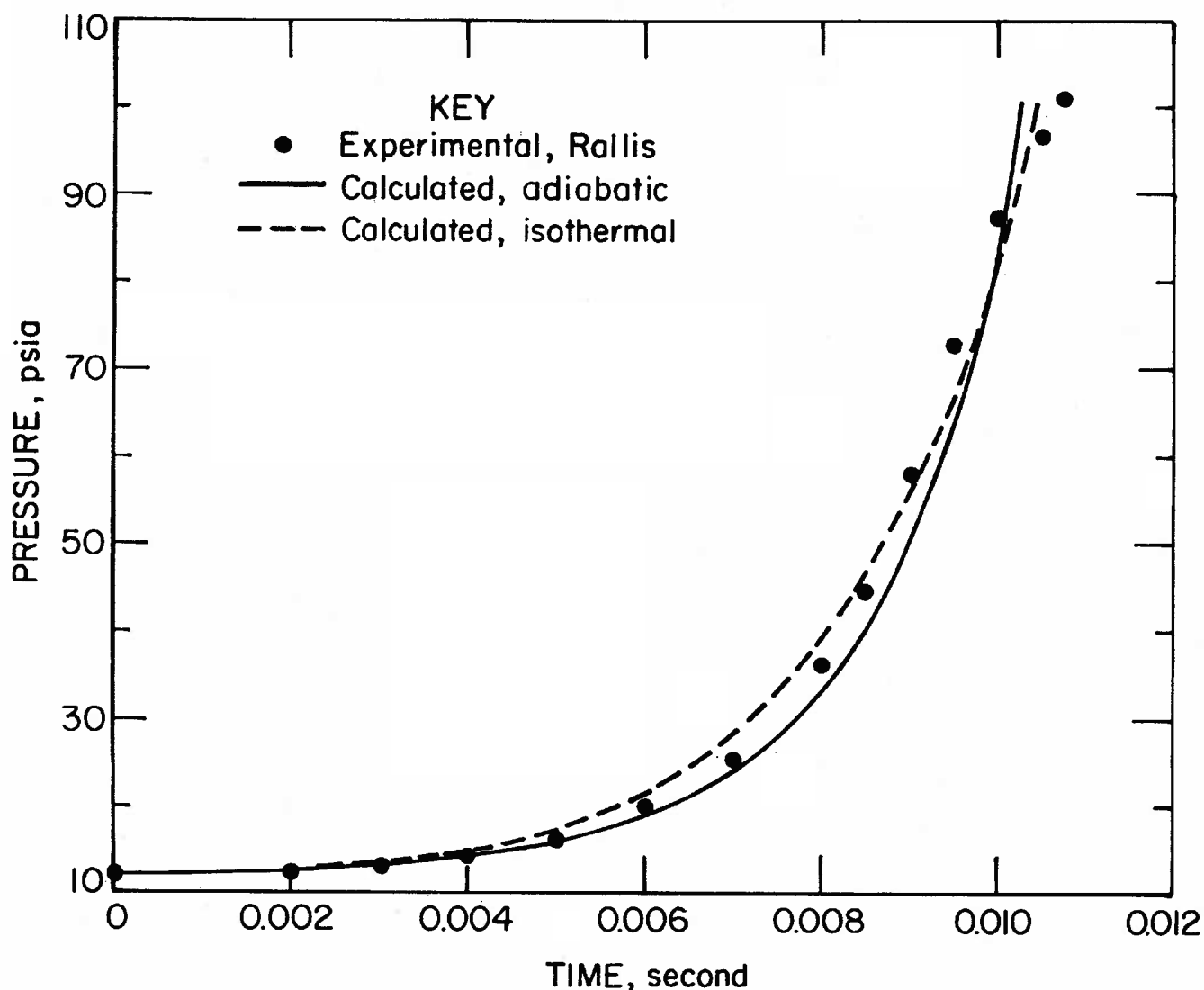


FIGURE 8. - Calculated and Experimental Data for Pressure and Time During a 7.72-Percent Acetylene-Air Explosion in a Spherical Vessel.

For the cornstarch explosion (adiabatic system), the values of  $\beta$  and  $k_r$  were obtained in the manner illustrated in figure 3. The value of 124 inches per second for  $k_r$  is an apparent rather than an actual value of burning velocity. Indications are that the size and shape of the vessel, as well as the initial turbulence induced when the dust is dispersed in the vessel, affect explosion development. Allowance for these factors must be made before the proper burning velocity can be calculated from the pressure-time data.

For the cornstarch test, the experimental values of time during the explosion are relative because zero time is not established accurately by instrumentation. For the previously reported gas explosion data, the values of time are those measured considering striking of the spark to be zero.

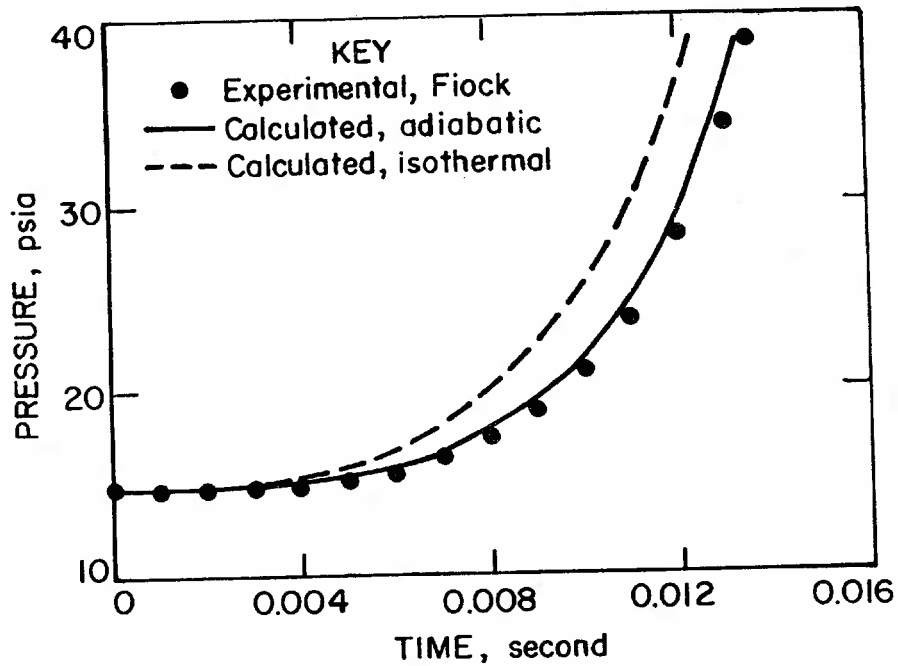


FIGURE 9. - Calculated and Experimental Data for Pressure and Time During a Moist Carbon Monoxide-Oxygen Explosion in a Spherical Vessel.

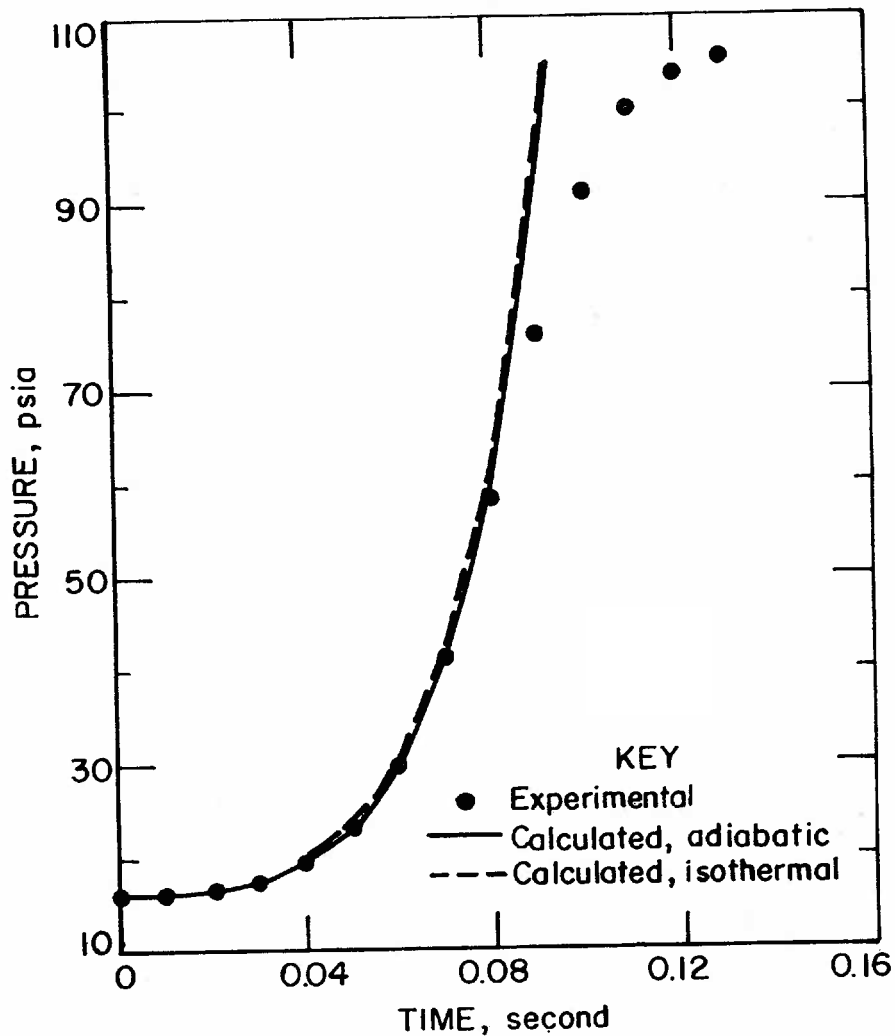


FIGURE 10. - Calculated and Experimental Data for Pressure and Time During an 0.8-oz/cu ft Cornstarch Dust Explosion in a 110-cu-ft Rectilinear Chamber.

## DISCUSSION

Equations are developed to correlate flame radius, pressure, and time for explosion in a spherical vessel. Indications are that the equations are adequate, within the limitations imposed by the simplifying assumptions, for both gas and dust explosions. Better agreement is obtained for the adiabatic than for the isothermal systems. However, it is anticipated that the simpler equations developed for the isothermal system should suffice in most applications. The development includes an empirical expression for the rate of reaction  $dn_b/dt$ , which appears to be consistent with observations for the soap-bubble and closed-vessel experiments.

Deviation of calculated from experimental value occurs primarily near the end of the explosion where, presumably, heat loss to the vessel walls becomes a factor. The developed model indicates that the rate of pressure rise increases in magnitude from the beginning to the end of the explosion when flame reaches the vessel wall. The experimental data show that a maximum rate of pressure rise exists ( $d^2P/dt^2 = 0$ ) when the flame has traveled about 95 per cent of the distance to the vessel wall.

Because of heat loss to the vessel wall and incomplete burning, the experimental maximum pressure is lower than the theoretical value. If the experimental value is used to calculate  $k_r$ , it will be higher than when calculated from the theoretical maximum pressure. For most gas explosion studies, a reasonable value of  $P_m$  can be calculated.

From the form of the differential and integrated equations for the pressure and time, it could be expected--as was observed in the calculations--that the constants  $\gamma$  and  $\beta$  as well as  $P_m$  and  $k_r$  are interrelated. Optimum values of  $\gamma$  and  $\beta$  as well as  $P_m$  and  $k_r$  were determined by trial calculation to produce relatively good agreement between equation and experiment. The chosen values of these constants appear to be reasonable.

In appendix B, isothermal and adiabatic values are given for  $k_r$  as calculated from equations 32 and 38, respectively. The adiabatic values of  $k_r$  for the gas explosions compare favorably with burning velocity values found in the literature, whereas the isothermal values are somewhat low. Evidence that the isothermal equations do not precisely fit gas explosion data is seen from the plotted flame radius-time and pressure-time curves; contrary to expectation, the isothermal explosions appear to be faster than the adiabatic. As shown in figure 10, both isothermal and adiabatic equations fit the dust explosion data. It is anticipated that most dust explosions may be treated as an isothermal process, and realistic values of  $k_r$  may be calculated using isothermal equation 32.

Mathematical relations between pressure, flame front, and time have been offered by a number of investigators. The final equations for an adiabatic system presented in this paper are similar to, but not the same as, those published by Lewis and von Elbe.<sup>21</sup> Introduction of the expression for the time-rate change of the burnt gas (equation 16) permits a straightforward derivation.

---

<sup>21</sup>Work cited in reference 17.

One empirical pressure-time relation appearing in the literature<sup>22</sup> shows  $P$  to be proportional to the cube of time, or

$$P = P_o + \frac{KP_o S_t^3 t^3}{V}. \quad (40)$$

This equation can be derived from equation 32 for the isothermal system in which  $\beta = 0$ , as follows:

$$\frac{dP}{dt} = \frac{3k_r T_o^2 P_m^{2/3}}{a T_r^2 P_o} (P_m - P_o)^{1/3} (P - P_o)^{2/3} P^{1/3}; \quad (41)$$

$$\text{letting } k_2 = \frac{k_r T_o^2 P_m^{2/3}}{a T_r^2 P_o} (P_m - P_o)^{1/3},$$

the equation becomes

$$\frac{dP}{(P - P_o)^{2/3} P^{1/3}} = 3k_2 dt. \quad (42)$$

When the left-hand side of equation 42 is expanded as a series and integrated, the pressure-time relation is

$$(P - P_o)^{1/3} - \frac{(P - P_o)^{4/3}}{12P_o} + \frac{2(P - P_o)^{7/3}}{63P_o^2} - \dots = P_o^{1/3} k_2 t. \quad (43)$$

for  $P_o \leq P \leq 2P_o$ .

The first term of this series has the same form as Zabetakis', and defines his coefficient of  $t^3$  to be

$$(P_m - P_o) \left( \frac{P_m}{P_o} \right)^2 \left( \frac{k_r T_o^2}{a T_r^2} \right)^3. \quad (44)$$

Calculations show little numerical difference between equations 32 and 40.

---

<sup>22</sup>Zabetakis, Michael G. Flammability Characteristics of Combustible Gases and Vapors. BuMines Bull. 627, 1965, 121 pp.

## APPENDIX A.--LIST OF SYMBOLS

- A - area of flame front, square inches.
- a - radius of vessel, inches.
- $k_r'$  - rate constant, inches per second.
- $k_r$  - reaction rate constant (burning velocity) at the reference level of temperature and pressure, inches per second.
- $k_1$  - constant -  $\frac{3\gamma k_r T_o^2 P_r^{\beta} P_m^{2/3\gamma}}{a T_r^2 P_o^{2-1/\gamma}} (P_m^{1/\gamma} - P_o^{1/\gamma})^{1/3}$ .
- $k_2$  - constant -  $\frac{k_r T_o^2 P_m^{2/3}}{a T_r^2 P_o} (P_m - P_o)^{1/3}$ .
- $\bar{M}$  - average molecular weight, pound per mole.
- m - total mass in vessel, pounds.
- n - number of moles.
- P - pressure, psia.
- R - universal gas constant,  $18,540 \frac{\text{lb in}}{\text{mole } ^\circ\text{Rankine}}$ .
- r - radius of flame front, inches.
- S - velocity, inches per second.
- T - temperature, degree Rankine.
- t - time, seconds.
- V - volume, cubic inches.
- x - linear dimension.
- X - algebraic variable.
- $\gamma$  - ratio of specific heat of a gas at constant pressure to that at constant volume.
- Superscript
- $\beta$  - exponent of pressure correlating transformation velocity with pressure.

Subscripts

- b - burnt zone.
- e - expansion (velocity), inches per second.
- i - initial (velocity), inches per second.
- m - final condition.
- n - mole change (velocity), inches per second.
- o - initial condition.
- r - condition at reference level.
- s - spatial (velocity), inches per second.
- t - transformation (velocity), inches per second.
- u - unburnt zone.

## APPENDIX B.--VALUE OF CONSTANTS USED IN CALCULATING EXPLOSION DATA

Constant	Acetylene-air		Carbon monoxide-oxygen		Cornstarch-air	
	Iso-thermal	Adiabatic	Isothermal	Adiabatic	Iso-thermal	Adiabatic
$\gamma$ .....	1	1.31	1	1.45	1	1.22
$\beta$ .....	0	.25	0	.27	0	.36
$k_r$ .....in/sec..	43	60	47	73	<sup>1</sup> 93	<sup>1</sup> 124
$T_o$ .....° R..	531	531	537	537	520	520
$T_r$ .....° R..	537	537	537	537	537	537
$P_o$ .....psia..	12.09	12.09	14.7	14.7	14.3	14.3
$P_r$ .....psia..	14.7	14.7	14.7	14.7	14.7	14.7
$P_m$ .....psia..	135.4	135.4	133.9	133.9	105.7	105.7
$a$ .....inches..	3.153	3.153	4.82	4.82	<sup>2</sup> 35.67	<sup>2</sup> 35.67

<sup>1</sup> An apparent value; effect of initial turbulence and pressure and vessel dimensions not considered.

<sup>2</sup> Experiment made in a rectilinear vessel having an equivalent spherical radius of 35.67 inches; the other experiments were made in spherical vessels.

# APPENDIX C.--CALCULATION OF PRESSURE-TIME AND RADIUS-TIME RELATIONS

Equations 37-38 for the adiabatic system were transformed to the following general form:

$$\int_0^{\chi} \frac{d\chi}{(A+B\chi^3)^{3-2\gamma+\gamma\beta}} = D \int_0^t dt.$$

The left integral was calculated using Simpson's rule; the values expressed in terms of  $\chi$  are shown in figures C-1 and C-2.

For equation 37,

$$\chi = r, A = 1, B = -\frac{1}{a^3} \left[ 1 - \left( \frac{P_o}{P} \right)^{1/\gamma} \right], \text{ and } D = \frac{k_r T_o^2 P_r \beta P_m^{1/\gamma}}{T_r^2 P_o^{1/\gamma+1}}.$$

For equation 38,

$$\chi = \left[ 1 - \left( \frac{P_o}{P} \right)^{1/\gamma} \right]^{1/3}, A = 1, B = -1,$$

$$\text{and } D = \frac{P_o^{2-2/\gamma-\beta}}{3\gamma} \frac{3\gamma k_r T_o^2 P_r \beta P_m^{2/3\gamma}}{a T_r^2 P_o^{2-1/\gamma}} (P_m^{1/\gamma} - P_o^{1/\gamma})^{1/3}.$$

The same general form is also used to evaluate equations 30 and 32 for the isothermal system; these data, considering  $\gamma = 1$  and  $\beta = \text{zero}$ , are also shown on figures C-1 and C-2. Through application of the curves in these figures, calculation of pressure-time and radius-time for a specific system is simplified. As a sample calculation (adiabatic system), equation 38 is applied to the acetylene-air data given in table 1. In this instance,  $A = 1$ ,  $B = -1$ , and

$$D = \frac{(12.09)^{2-2/1.31-0.25}}{(3)(1.31)} \cdot \frac{(3)(1.31)(60)(531)^2(14.7)^{0.25}(135.4)^2/(3)(1.31)}{(3.153)(537)^2(12.09)^{2-1/1.31}}$$

$$\cdot [(135.4)^{1/1.31} - (12.09)^{1/1.31}]^{1/3},$$

or  $D = 114$ . Hence, when  $P = 30$  psia,

$$\chi = \left[ 1 - \left( \frac{12.09}{30} \right)^{1/1.31} \right]^{1/3} = 0.793.$$

Therefore,

$$\int_0^{\chi} \frac{d\chi}{(1-0.793^3)^{3-2(1.31)} + 1.31(0.25)} = 114 \text{ t.}$$

From figure C-2, curve 2, the value of this integral for  $\chi = 0.793$  is 0.89. Hence, the time when  $P = 30$  psia is

$$t = \frac{0.89}{114} = 0.0078 \text{ second.}$$

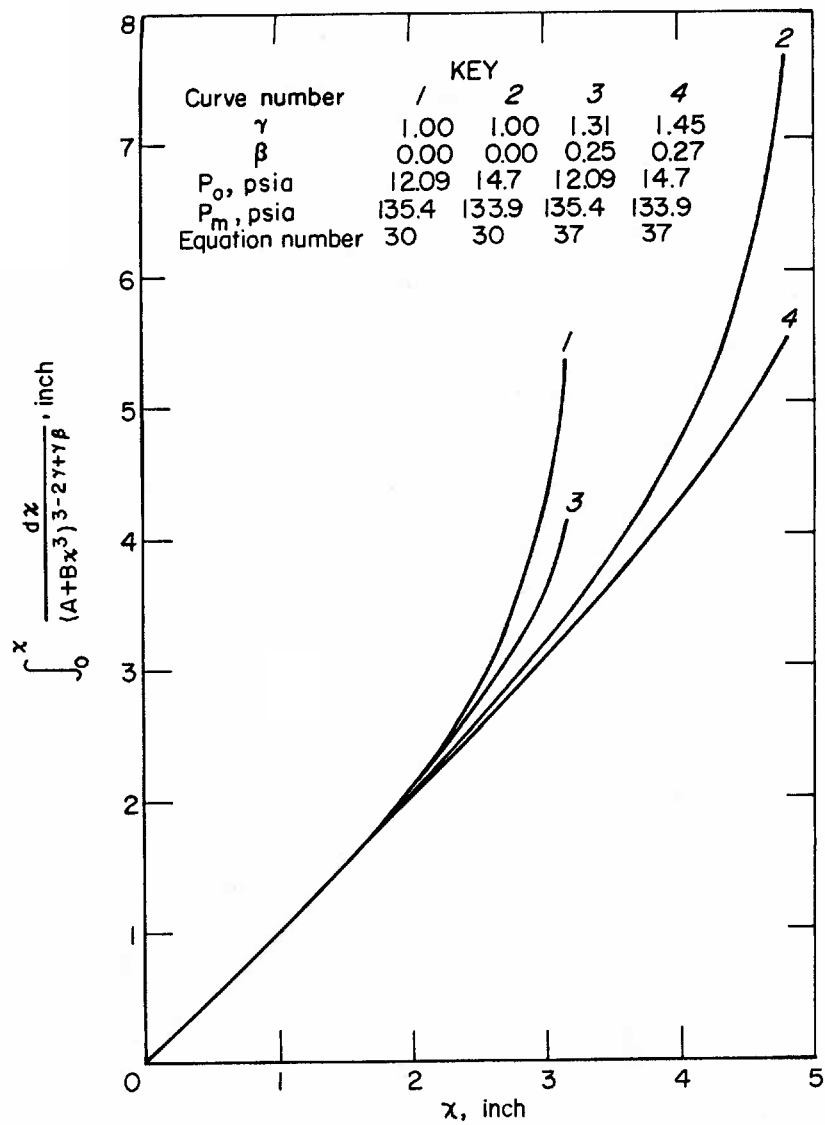


FIGURE C-1. - Integral Evaluation by Simpson's Rule for Equations 30 and 37.

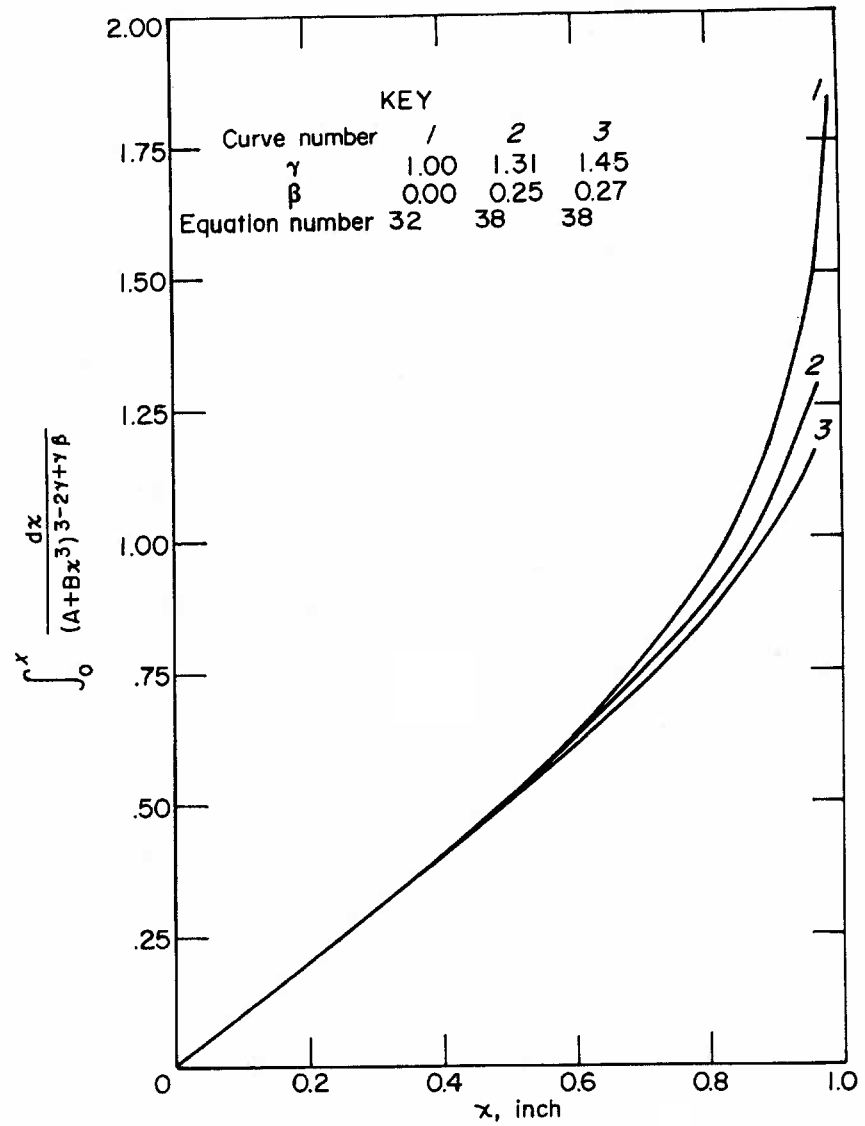


FIGURE C-2. - Integral Evaluation by Simpson's Rule for Equations 32 and 38.